

Ultra-short echo time magnetic resonance angiography using a modified signal targeting with alternative radio frequency spin labeling technique for detecting recanalized pulmonary arteriovenous malformation after coil embolization

Acta Radiologica Open
10(10) 1–6
© The Author(s) 2021
Article reuse guidelines:
sagepub.com/journals-permissions
DOI: 10.1177/20584601211057671
journals.sagepub.com/home/arr


Kohei Hamamoto^{1,2} , Emiko Chiba³, Noriko Oyama-Manabe², and Hiroshi Shinmoto¹

Abstract

Pulmonary arteriovenous malformation (PAVM) is a rare vascular anomaly, for which transcatheter embolization with metallic coils is the standard of care. Although detecting recanalization after embolotherapy is crucial, direct visualization of residual flow with computed tomography or magnetic resonance (MR) imaging is generally difficult due to metal artifacts. We present a case of recanalized PAVM after coil embolization detected by ultra-short echo time MR angiography using a modified signal targeting with an alternative radio frequency spin labeling technique.

Keywords

pulmonary arteriovenous malformation, signal targeting alternating radio frequency with asymmetric inversion slabs, ultra-short echo time, non-contrast-enhanced magnetic resonance angiography

Received 25 May 2021; Accepted 18 October 2021

Introduction

Pulmonary arteriovenous malformations (PAVMs) are rare pulmonary vascular structures with direct communication between the pulmonary artery and pulmonary vein circulations through a thin-walled sac.^{1,2} Embolotherapy with metallic coils is considered as the standard treatment for PAVM.^{2,3} However, a major concern of embolotherapy is recanalization, in which some patients develop neurological events.^{4,5}

Digital subtraction angiography (DSA) is the most reliable modality for detecting recanalization, although it is not routinely performed because of its invasiveness. In recent years, non-invasive techniques, such as computed tomography (CT) and magnetic resonance imaging (MRI), with or without contrast agents, have been used to detect the presence of PAVM recanalizations^{6–12}. However, direct

visualization of recanalizations with CT and MRI is limited because of the prominent streak or susceptibility artifacts induced by metallic coils. Herein, we described a case of recanalized PAVM treated by coil embolization detected by ultra-short echo time magnetic resonance angiography using a modified signal targeting with alternative radio

¹Department of Radiology, National Defense Medical College, Tokorozawa, Saitama, Japan

²Department of Radiology, Jichi Medical University Saitama Medical Center, Omiya-ku, Saitama, Japan

³Department of Radiology, National Center Hospital, National Center of Neurology and Psychiatry, Kodaira, Tokyo, Japan

Corresponding author:

Kohei Hamamoto Department of Radiology, National Defense Medical College, 3-2 Namiki, Tokorozawa, Saitama, 359-8513, Japan.
Email: hkouhei917@gmail.com



Creative Commons Non Commercial CC BY-NC: This article is distributed under the terms of the Creative Commons Attribution-NonCommercial 4.0 License (<https://creativecommons.org/licenses/by-nc/4.0/>) which permits non-commercial use, reproduction and distribution of the work without further permission provided the original work is attributed as specified on the SAGE and Open Access pages (<https://us.sagepub.com/en-us/nam/open-access-at-sage>).

frequency spin labeling technique (UTE-ASTAR MRA), in which no susceptibility artifacts were detected.

Case Report

A 63-year-old woman with multiple PAVMs (eight lesions) in the bilateral lung concomitant with hereditary hemorrhagic telangiectasia was referred to our hospital for endovascular treatment. Transcatheter embolization of the feeding arteries and/or sacs with platinum and stainless-steel coils was performed in multiple sessions, resulting in the complete occlusion of each PAVM. A follow-up unenhanced CT scan 4 months later revealed that the shrinkage rates of the diameters of the draining veins of the two PAVMs in segment 4 of the right middle lobes treated with platinum coils were 48% and 45%, respectively, indicating the recanalization of these PAVMs.¹¹ However, it was difficult to visualize and evaluate the continuity between the feeding artery, sac, and draining vein because of severe streak artifacts induced by the metallic coils (Figure 1(a)).

To further evaluate the recanalization, we performed UTE MRI, UTE-ASTAR MRA, and time-resolved contrast-enhanced magnetic resonance angiography (TR-CEMRA) using a 3.0-T MRI system (Vantage Titan 3T, Canon Medical Systems, Tochigi, Japan). The MRI parameters are presented in Table 1. Although the detailed algorithm for ASTAR has not been disclosed, the arterial spin labeling (ASL) technique was used as a preparation pulse,¹³ which provided multi-phase MRA images during one session. An overview of the image acquisition of the UTE-ASTAR MRA is shown in Figure 2. For the UTE-ASATR MRA, respiratory triggering was applied at the beginning of expiration. Due to the limited acquisition volume of UTE-ASTAR MRA, we set the position of each slab to include the feeding artery, sac, and draining vein along with portions of the main pulmonary artery and vein of the target PAVMs according to the UTE MRI scans.

For the UTE MRI, the continuity of the feeding artery, sac, and draining vein were visualized as high signal intensities in both treated PAVMs (Figure 1(b)). However, it was difficult to distinguish whether these signals were actual blood flow or thrombi. Thus, UTE-ASTAR MRA provided serial hemodynamic images and clearly visualized the blood flow signals inside the coils and the continuity of the feeding artery, sac, and draining vein (Figures 1(c) to (e)). In contrast, in the untreated lung field, only the pulmonary arteries were visualized, even at 816 ms. On TR-CEMRA, the feeding artery and draining vein of the treated PAVMs were simultaneously visualized in the pulmonary arterial phase (Figure 1(f)). Based on these findings, recanalization through the coils in the PAVMs in the right middle lobe was suggested. DSA performed in the secondary embolization revealed recanalization through the coils placed in the feeding arteries of both treated PAVMs (Figures 3(a) and

(b)). These findings were consistent with those of UTE-ASTER MRA (Figures 3(c) and (d)). An additional platinum coil embolization of the recanalized lumen was performed.

Discussion

In the present case, UTE-ASTAR MRA provided hemodynamic information using the ASL technique and enabled clear visualization of the continuity through the embolized coils from the feeding artery to the draining vein. These findings are similar to those of DSA.

Although it is important to evaluate the prevalence of recanalization because it can occur in up to 50% of embolotherapy patients and may cause neurologic events after embolization of PAVMs,^{4,5} the direct diagnosis of recanalization of PAVMs with CT or MRI remains a challenge. Recently, the utility of UTE MRI in the detection of PAVM recanalization has been reported.¹⁴ This method visualizes the continuity through the embolized coils from the feeding artery to the draining vein, but physicians might misinterpret static tissues, including thrombi in coils and sacs as lesions, given their high signal intensity. Therefore, imaging modalities that provide hemodynamic information in addition to UTE MRI remain necessary to evaluate recanalization. UTE-ASTAR MRA could provide useful information for the non-invasive definitive diagnosis of recanalization. To the best of our knowledge, this is the first report demonstrating the utility of UTE with ASL in the detection of PAVM recanalization after metallic coil embolization.

Similar to the present report, several clinical studies have reported that UTE with ASL reduces the artifacts typically observed after coil or stent placement in intracranial lesions.^{15–17} However, applying this technique in evaluating vascular lesions in the body, such as PAVMs, remains challenging given that additional techniques, including respiratory and/or electrocardiogram synchronization, are required to acquire images of the body trunk. Recently, Mori et al. reported the utility of UTE MRA with time-spatial labeling inversion. Their method used the ASL technique with deep learning reconstruction for the assessment of a renal artery aneurysm treated with metallic coils.¹⁸ This method enabled visualization of the blood flow signals adjacent to the placed metallic coils, which was similar to our case, but it still did not provide serial hemodynamic images similar to those of UTE-ASTAR MRA or DSA. As described above, the continuous visualization of the feeding artery, sac, and draining vein through the placed coils is crucial to achieve a definitive diagnosis of recanalization. Therefore, UTE-ASTAR MRA might be more suitable for assessing recanalization of embolized PAVMs.

It is notable that UTE-ASTAR MRA can provide high temporal resolution similar to those of hemodynamic

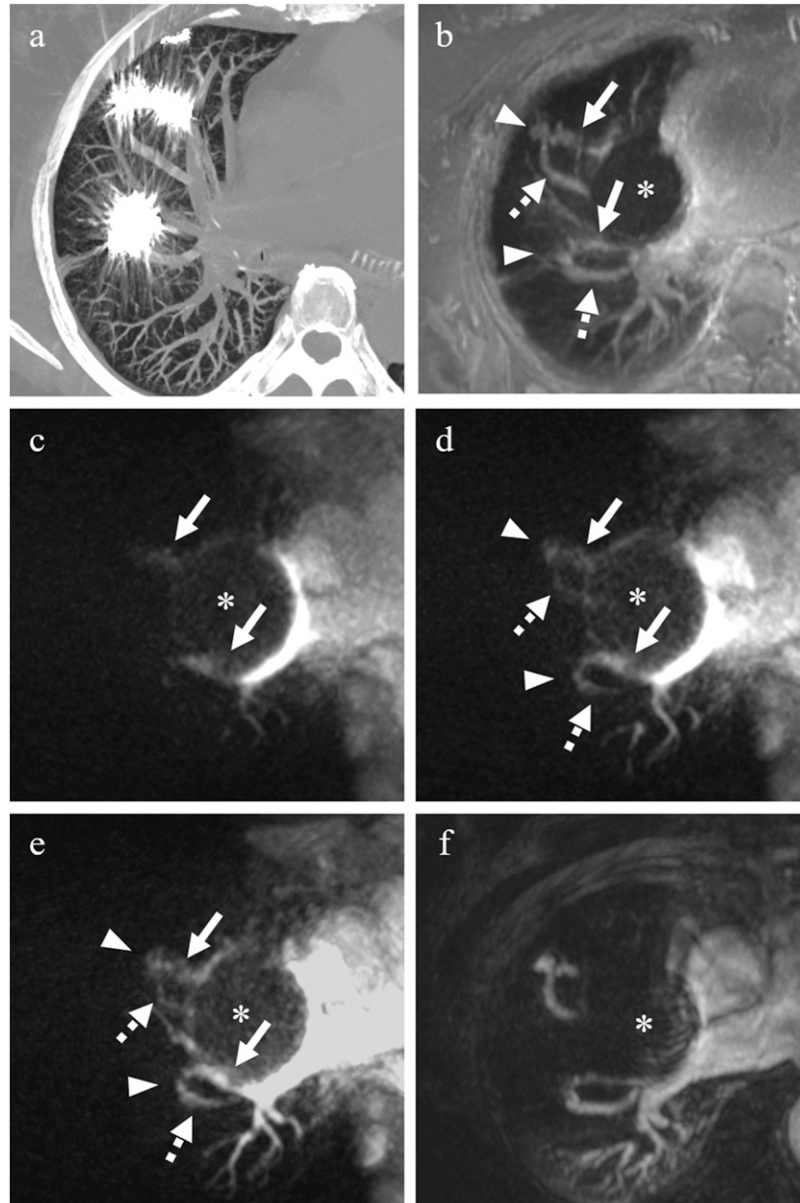


Figure 1. Evaluation of recanalization after the embolization of a pulmonary arteriovenous malformation (PAVM). (a) Unenhanced computed tomography with partial maximum intensity projection (MIP) for image evaluation around the placed coils is difficult to interpret due to the prominent streak artifact from the coils. The platinum coils were placed in the feeding artery of the anterior lesion and in the sac of posterior lesion. (b) Ultra-short echo time magnetic resonance image (UTE MRI) with partial MIP showing the continuity of the lateral feeding arteries (arrows), sac (arrowheads), and draining vein (dashed arrows) in both embolized PAVM. (c–e) UTE MR angiography using a modified signal targeting with alternative radio frequency spin labeling technique (UTE-ASTAR MRA). The images were presented with partial MIP. The delay time of images (c), (d), and (e) was 200, 506, and 812 ms, respectively. On the UTE-ASTAR MRA, the continuity of the feeding arteries (arrows), sacs (arrowheads), and draining veins (dashed arrows) were serially visualized from 200 to 812 ms in both PAVMs. Note that the blood signals were visualized in the placed coils. (f) Time-resolved contrast-enhanced MRA. Asterisks in (b)–(f) indicate the image distortion due to the magnetic susceptibility artifact from stainless-steel coils placed in the PAVM adjacent to target lesions.

images at 300 ms intervals without contrast medium. Generally, the temporal resolutions of DSA and TR-CEMRA are approximately 100 ms and 2000 ms, respectively. Our method, which has a suitable temporal resolution

comparable to that of DSA, was superior to TR-CEMRA in detecting recanalized PAVMs. In addition, it was also useful for the initial diagnosis of PAVMs and therapeutic effect even in other body lesions treated with metallic devices,

Table I. Magnetic resonance imaging parameters.

	UTE MRI	UTE-ASTAR MRA	TR-CEMRA
TE/TR (ms)	0.096/3.7	0.100/3.0	1.3/3.7
Flip angle (°)	5	5	20
Slice thickness (mm)	1	1 ^a	1.25 ^b
Slice section (n)	200 (to cover the entire lung field)	160 (to cover the embolized lesions)	40 (to cover the embolized lesions)
Field of view (mm)	480 × 480	350 × 350	370 × 370
Matrix size	512 × 512	512 × 512 ^c	512 × 320 ^c
Signal acquired (n)	1	2	1
Parallel imaging acceleration factor	N/A	1	2
Acquisition voxel size (mm)	0.94 × 0.94 × 1	0.68 × 0.68 × 1	0.72 × 1.16 × 1.25
Imaging time	7 min 50 s	12 min 30 s	30 s

^aThe acquired slice sections of 2 mm were reconstructed with 1.0-mm voxel intervals by mid-slice reconstruction.

^bThe acquired slice sections of 2.5 mm were reconstructed with 1.25-mm voxel intervals by mid-slice reconstruction.

^cReconstruction matrix.

N/A, not applicable; UTE MRI, ultra-short echo time magnetic resonance imaging; UTE-ASTAR MRA, ultra-short echo time magnetic resonance angiography using a modified signal targeting with alternative radio frequency spin labeling technique; TR-CEMRA, time-resolved contrast-enhanced magnetic resonance angiography; TR, repetition time; TE, echo time.

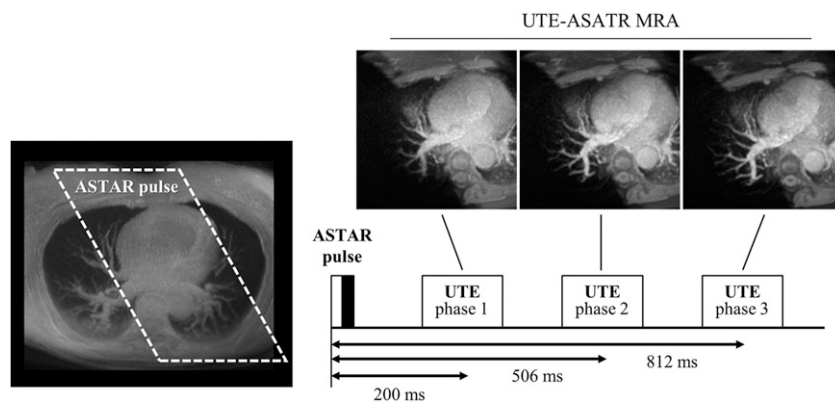


Figure 2. Procedure for acquiring UTE-ASTAR MRA. Three-dimensional UTE images were serially acquired at 200, 506, and 812 ms of delay time after applying the ASTAR pulse. The ASTAR pulse (tag) was placed on the range that covered the right ventricle and main trunk of the pulmonary artery in the axial direction (dashed parallelogram). Note that the peripheral portion of the pulmonary arteries in the left lung field is gradually visualized from phase 1 to phase 3 on UTE-ASTAR MRA.

including coils and stents. Indeed, we confirmed that UTE-ASTAR MRA could provide hemodynamic images in untreated PAVMs and detect residual blood flow in visceral artery aneurysms treated with platinum coils (unpublished data).

UTE-ASTAR MRA has additional advantages over contrast-enhanced CT and TR-CEMRA. First, this method does not require exposure to ionizing radiation or iodine- or gadolinium-based contrast agents, which may result in nephrotoxicity, anaphylaxis, nephrogenic systemic fibrosis, and tissue deposition of gadolinium. This might be particularly useful for young and/or pregnant patients with PAVM who require regular follow-up over an extended period. Second, UTE-ASTAR MRA has a relatively briefer acquisition window in the late expiration phase, which was

triggered by respiratory gating results in reduction-in-motion artifacts, compared with the settings of TR-CEMRA.

Despite these advantages, UTE-ASTAR MRA has some limitations compared to TR-CEMRA and CT. First, the acquisition time of UTE-ASTAR MRA was approximately 10–12 min, which was much longer than that of TR-CEMRA and CT. Second, UTE-ASTAR MRA had limits on the number of acquisitions in a single session, and therefore it was difficult to cover the entire lung field with high spatial resolution during a single session. However, given that there was no time constraint with UTE-ASTAR MRA, the image of the entire lung field could be acquired by planning multiple sessions. Third, the spatial resolution of UTE-ASTAR MRA is relatively low compared with that

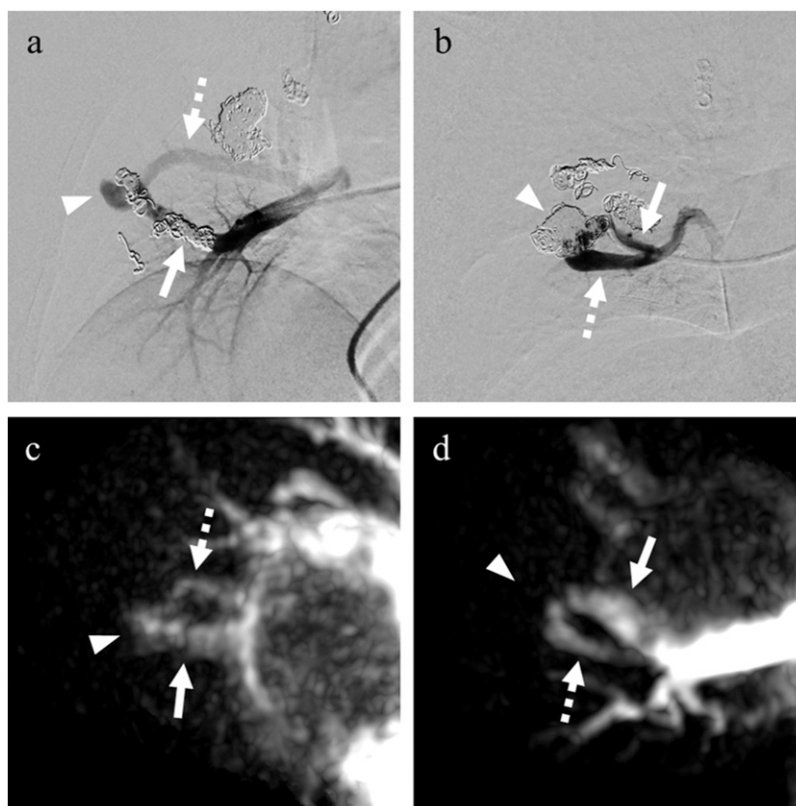


Figure 3. Digital subtraction angiography (DSA) during the second embolotherapy for the recanalized PAVM. (a) Anterior lesion. (b) Posterior lesion. The recanalization through the previously placed coils was confirmed in both lesions. Arrows, arrowhead, and dashed arrows indicate the feeding arteries, sacs, and draining veins, respectively. (c), (d) The partial MIP images of UTE-ASTAR MRA at the views corresponding to DSA images.

of CT, owing to the susceptibility to artifacts and limitations of slice thickness imposed by the available equipment. This drawback may be avoided using a higher magnetic-field MR imaging scanners that can achieve higher signal-to-noise ratios or using a newly developed deep learning reconstruction. Finally, the capability of UTE-ASTAR MRA to detect minor signals from residual flow might depend on the packing density and material of the coils. In this case, severe image distortion could occur around the stainless-steel coils. Therefore, the application of UTE-ASTAR MRA for lesions treated with stainless-steel coils might be limited.

In conclusion, the present report suggests that UTE-ASTAR MRA is a useful method for detecting recanalization of PAVMs after coil embolization without contrast injection and radiation exposure.

Acknowledgements

This research received no specific grant from any funding agency in the public, commercial, or not-for-profit sectors. We thank Yoshimasa Ikeda and Yusuke Ayabe for their technical advice regarding magnetic resonance imaging.

Declaration of conflicting interests

The author(s) declared no potential conflicts of interest with respect to the research, authorship, and/or publication of this article.

Funding

The author(s) received no financial support for the research, authorship, and/or publication of this article.

ORCID iD

Kohei Hamamoto  <https://orcid.org/0000-0002-7430-1944>

References

1. Remy J, Remy-Jardin M, Wattinne L, et al. Pulmonary arteriovenous malformations: evaluation with CT of the chest before and after treatment. *Radiology* 1992; 182: 809–816.
2. White RI Jr, Pollak JS, Wirth JA. Pulmonary arteriovenous malformations: diagnosis and transcatheter embolotherapy. *J Vasc Interv Radiol* 1996; 7: 787–804.
3. Mager JJ, Overtoom TT, Blauw H, et al. Embolotherapy of pulmonary arteriovenous malformations: long-term results in 112 patients. *J Vasc Interv Radiol* 2004; 15: 451–456.

4. Lee DW, White RI Jr, Egglin TK, et al. Embolotherapy of large pulmonary arteriovenous malformations: longterm results. *Ann Thorac Surg* 1997; 64: 930–939.
5. Milic A, Chan RP, Cohen JH, et al. Reperfusion of pulmonary arteriovenous malformations after embolotherapy. *J Vasc Interv Radiol* 2005; 16: 1675–1683.
6. Remy-Jardin M, Dumont P, Brillet PY, et al. Pulmonary arteriovenous malformations treated with embolotherapy: helical CT evaluation of long-term effectiveness after 2–21-year follow-up. *Radiology* 2006; 239: 576–585.
7. Fidelman N, Gordon RL, Bloom AI, et al. Reperfusion of pulmonary arteriovenous malformations after successful embolotherapy with vascular plugs. *J Vasc Interv Radiol* 2008; 19: 1246–1250.
8. Woodward CS, Pyeritz RE, Chittams JL, et al. Treated pulmonary arteriovenous malformations: patterns of persistence and associated retreatment success. *Radiology* 2013; 269: 919–926.
9. Makimoto S, Hiraki T, Gobara H, et al. Association between reperfusion and shrinkage percentage of the sac after embolization of pulmonary arteriovenous malformation: evaluation based on contrast-enhanced thin-section CT images. *Jpn J Radiol* 2014; 32: 266–273.
10. Bousset L, Cernicanu A, Geerts L, et al. 4D time-resolved magnetic resonance angiography for noninvasive assessment of pulmonary arteriovenous malformations patency. *J Magn Reson Imaging* 2010; 32: 1110–1116.
11. Kawai T, Shimohira M, Kan H, et al. Feasibility of time-resolved MR angiography for detecting recanalization of pulmonary arteriovenous malformations treated with embolization with platinum coils. *J Vasc Interv Radiol* 2014; 25: 1339–1347.
12. Hamamoto K, Matsuura K, Chiba E, et al. Feasibility of Non-contrast-enhanced MR Angiography Using the Time-SLIP Technique for the Assessment of Pulmonary Arteriovenous Malformation. *Magn Reson Med Sci* 2016; 15: 253–265.
13. Takakura K, Kido A, Fujimoto K, et al. Evaluation of appropriate readout sequence for renal MRI perfusion using ASTAR (ASL) technique. *Nihon Hoshasen Gijutsu Gakkai Zasshi* 2016; 72: 1105–1112.
14. Hamamoto K, Chiba E, Matsuura K, et al. Ultra-short echo time magnetic resonance imaging for detection of pulmonary arteriovenous malformation recanalization after coil embolization: a case report and a phantom study. *Acta Radiol Open* 2017; 6: 2058460117732101.
15. Gönner F, Heid O, Remonda L, et al. MR angiography with ultrashort echo time in cerebral aneurysms treated with Guglielmi detachable coils. *Am J Neuroradiol* 1998; 19: 1324–1328.
16. Gönner F, Lövblad KO, Heid O, et al. Magnetic resonance angiography with ultrashort echo times reduces the artefact of aneurysm clips. *Neuroradiology* 2002; 44: 755–758.
17. Irie R, Suzuki M, Yamamoto M, et al. Assessing blood flow in an intracranial stent: A feasibility study of MR angiography using a silent scan after stent assisted coil embolization for anterior circulation aneurysms. *Am J Neuroradiol* 2015; 36: 967–970.
18. Mori R, Kassai Y, Masuda A, et al. Ultrashort echo time time-spatial labeling inversion pulse magnetic resonance angiography with denoising deep learning reconstruction for the assessment of abdominal visceral arteries. *J Magn Reson Imaging* 2020. DOI: [10.1002/jmri.27481](https://doi.org/10.1002/jmri.27481).